# Sub-grid scale modeling of the equation of state for fully compressible combustion LES

**By G. Ribert†, P. Domingo† AND L. Vervisch†**

In large-eddy simulations (LES) of multicomponent and fully compressible flows, the pressure is formally obtained after filtering the equation of state. In practice, correlations between density, species and temperature are usually neglected to compute the filtered pressure from the resolved fields. Analyzing one-dimensional and three-dimensional $H_2/O_2$ space-filtered flames, we have found that a large part of the error introduced by the linearization of the equation of state can be counterbalanced by expressing the mean molar weight of the mixture with the Reynolds filtered species mass fractions, instead of the density-weighted mass fractions. An approximate deconvolution/filtering procedure is then discussed to estimate the Reynolds filtered mass fractions from the density-weighted mass fractions, which are the transported quantities in LES flow solvers.

## 1. Introduction

Modern computing facilities performing well-resolved flow simulations allow us to revisit some classic modeling assumptions in order to accurately describe flow physics. In the simulations of turbulent flames, the modeling of the interactions between flow turbulence, thermodynamics and chemistry are a very sensitive point. Neglecting the effects induced by unresolved fluctuations of the species concentrations and of the temperature cannot be an option in the context of high-fidelity simulations. Along these lines, the treatment of the equation of state (EoS) in fully compressible large-eddy simulation (LES) has not been addressed in detail so far.

The filtering of the EoS provides the filtered pressure in a fully compressible LES. Correlations between species, mass fractions and temperature are usually neglected to simply express the filtered pressure directly from the knowledge of the density-weighted filtered species mass fractions and temperature. A formulation that may be valid is the case where a species concentration dominates the mixture, for instance nitrogen, but fails in the particular case of oxy-combustion. Even in the case of a binary mixture, Selle *et al.* (2007) illustrated how the error, due to linearization of the filtered EoS, grows with the filter size.

This issue is further examined by filtering a one-dimensional freely propagating premixed $H_2/O_2$ flame and a three-dimensional turbulent slot burner simulated with detailed chemistry. The filtering of the EoS is analyzed, and an approximate deconvolution/filtering procedure, which significantly reduces the remaining contribution of the unresolved sub-grid scale (SGS) part, is discussed.

† CORIA / INSA de Rouen, France

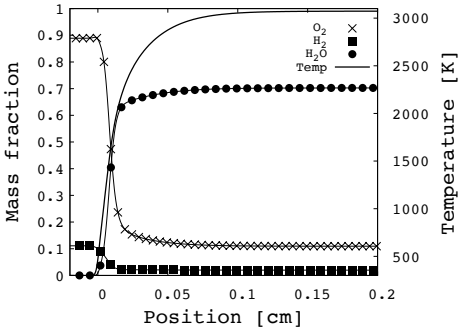


(a) Major species and temperature

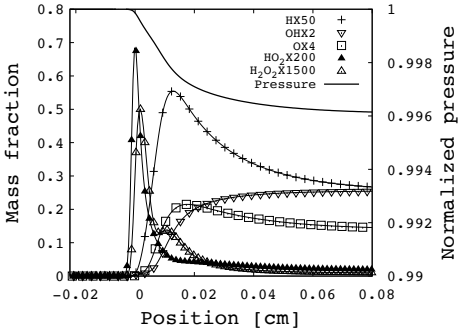


(b) Minor species and pressure

FIGURE 1. One-dimensional stoichiometric $H_2/O_2$ freely propagating premixed flame.

## 2. Problem formulation

The EoS for an ideal or non-ideal gas composed of $n$ chemical species may be written in a generic form as a function of the partial densities, $\rho_i$, and temperature, $T$

$$P = P(\rho_1, \cdots, \rho_n, T)\,. \tag{2.1}$$

In the simple case of an ideal gas

$$P = R\left(\sum_{i=1}^{n} \frac{\rho_i}{W_i}\right) T = \rho R \left(\sum_{i=1}^{n} \frac{Y_i}{W_i}\right) T = \rho r_{\text{Mix}} T\,, \tag{2.2}$$

where $Y_i$ is the mass fraction and $W_i$ is the molar weight of the $i$-th species. $R$ is the universal gas constant and $r_{\text{Mix}} = \left(\sum_{i=1}^{n} Y_i/W_i\right) R = R/W$ the gas constant of the mixture and $W = \left(\sum_{i=1}^{n} Y_i/W_i\right)^{-1}$ the species averaged molar weight. Filtering this EoS leads to

$$\overline{P} = R\left(\frac{\overline{\rho T Y_1}}{W_1} + \cdots + \frac{\overline{\rho T Y_n}}{W_n}\right)\,. \tag{2.3}$$

Today, in most fully compressible flow solvers, it is assumed that correlations between

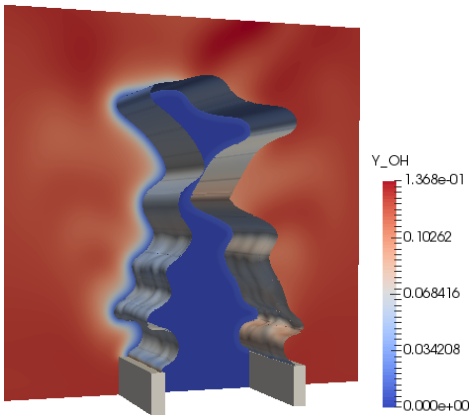


FIGURE 2. Snapshot of the stoichiometric $H_2/O_2$ slot burner turbulent premixed flame.

species concentrations and temperature can be neglected when filtering the EoS

$$\overline{\rho Y_i T} = \overline{\rho}\widetilde{Y_i T} \approx \overline{\rho}\widetilde{Y}_i\widetilde{T}\,, \tag{2.4}$$

where the usual Favre filtering is introduced ($\widetilde{T} = \overline{\rho T}/\overline{\rho}$ and $\widetilde{Y}_i = \overline{\rho Y}_i/\overline{\rho}$). This assumption may be valid when a diluent (usually nitrogen) dominates the gas composition, i.e., $Y_{N_2} >> Y_i\ \forall i \neq N_2$. Then the dominant nitrogen term assumes in Eq. (2.3) that $\overline{P} \approx \overline{\rho T} R(\widetilde{Y}_{N_2}/W_{N_2}) = \overline{\rho} r_{\mathrm{Mix}} \widetilde{T}$, with $r_{\mathrm{Mix}} = R(\widetilde{Y}_{N_2}/W_{N_2})$ roughly constant. This assumption of weak variations of the mean molar weight may not be valid on the rich side of non-premixed air-flames or at any flow location in the case of oxy-flames.

## 3. Canonical flames studied

Two canonical flows are examined to study space filtering of the EoS. The fully compressible SiTCom-B flow solver is used, in which the convective terms are computed resorting to a fourth-order centered skew-symmetric-like scheme (Ducros *et al.* 2000), the diffusive terms are discretized with a fourth-order centered scheme, time is advanced with a third-order Runge-Kutta method (Gottlieb & Shu 1998) and the boundary conditions are prescribed with 3D-NSCBC (Lodato *et al.* 2008).

The first reacting flow is a one-dimensional premixed flame freely propagating in a stoichiometric mixture of $H_2/O_2$. The chemistry is described for eight species, $O_2$, $H_2$, $H_2O$, H, OH, O, $HO_2$, $H_2O_2$, involved in 21 elementary reactions (Williams 2008). The transport coefficients are expressed with a mixture-average formulation (Curtiss & Hischfelder 1949). For a resolution of 5 µm, Figure 1 shows the distribution of major and minor species and temperature across the flame. The flame speed is $S_L = 10$ m/s and the thermal flame thickness based on the temperature gradient is of the order of 200 µm.

The second reacting flow is a three-dimensional turbulent premixed flame developing downstream of a slot burner (Figure 2). The bulk velocity of the premixed jet is 70 m/s and its temperature is 300 K. The temperature of the coflowing burnt gases is 3080 K and the bulk velocity of this stream is 15 m/s. Velocity fluctuations are added to the injected mean flow, according to a synthetic homogeneous turbulence with $u'/S_L = 2.1$, thus leading to a moderate level of flame wrinkling because of the high value of the oxy-flame speed, even though 30% of turbulence is injected. Large-scale pulsations in the streamwise direction are also observed in these simulations. The structured mesh

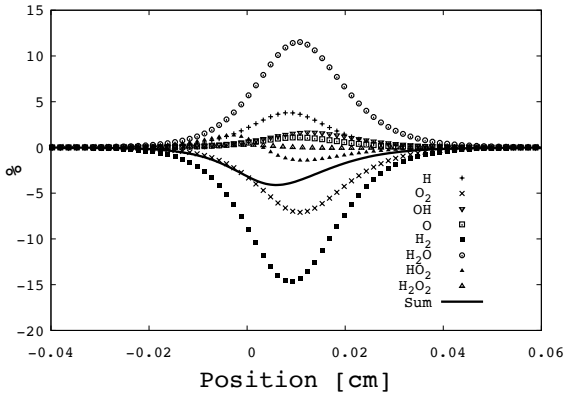


FIGURE 3. Distribution of $R(\overline{\rho TY_i} - \overline{\rho}\widetilde{T}\widetilde{Y}_i)/(W_i\overline{P})$ (%) in a one-dimensional flame. *A-priori* filtering with a filter size $\Delta = 300$ μm.

is composed of 200M cells with a resolution of 6.25 μm. A wrinkled premixed flame surface is observed, with the eventual formation of isolated pockets of burnt gases at the turbulent flame tip.

## 4. Analysis of EoS filtering

Expressing the EoS in the linearized form, as usually done,

$$\overline{P} = R\left(\frac{\overline{\rho}\widetilde{T}\widetilde{Y}_1}{W_1} + \cdots + \frac{\overline{\rho}\widetilde{T}\widetilde{Y}_n}{W_n}\right), \tag{4.1}$$

implies that the SGS contribution

$$R\sum_{i=1}^{n}\frac{1}{W_i}\left(\overline{\rho TY_i} - \overline{\rho}\widetilde{T}\widetilde{Y}_i\right) \tag{4.2}$$

stays small compared with the filtered pressure.

Filtered quantities are obtained in the one-dimensional flame and the three-dimensional DNS by applying an approximate and discretized form of a Gaussian filter (Sagaut 2001; Katopodes *et al.* 2004)

$$\overline{Y}_i = Y_i + \frac{\Delta^2}{24}\nabla^2\overline{Y}_i\,, \tag{4.3}$$

in which an implicit formulation is chosen to secure stability and facilitate deconvolution introduced thereafter.

Figure 3 shows the distribution through the one-dimensional flame of

$$R(\overline{\rho TY_i} - \overline{\rho}\widetilde{T}\widetilde{Y}_i)/(W_i\overline{P}) \tag{4.4}$$

for every species and its sum over all the chemical species. A filter size $\Delta = 300$ μm is used. $H_2O$, H, OH and O have a positive contribution to the SGS term, up to 12% for $H_2O$ while other species of this group contribute less than 5%. The SGS term of $HO_2$ and $H_2O_2$ is of the order of a few % with a change of sign across the reaction zone. $O_2$

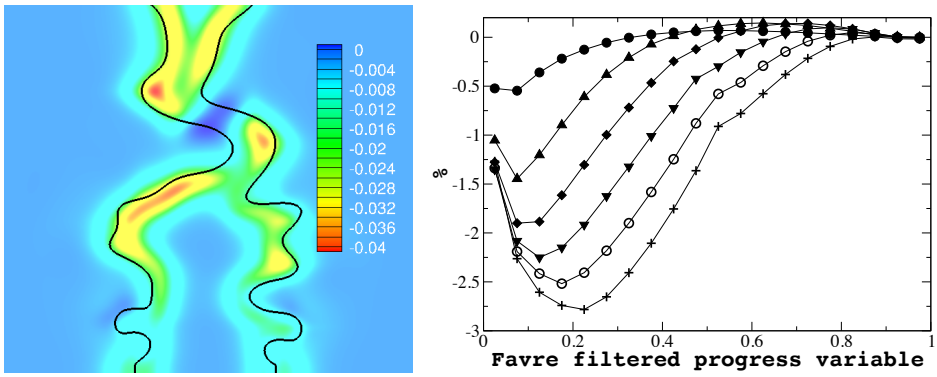


(a) Snapshot in a transverse plane (b) $\langle P^{\star}_{\mathrm{SGS_{EoS}}} | \widetilde{c} \rangle \times 100$

FIGURE 4. $P^{\star}_{\mathrm{SGS_{EoS}}} = \left( \overline{P} - \overline{\rho} R \widetilde{T} \sum_i (\widetilde{Y}_i / W_i) \right) / \overline{P}$. (a) Black line: iso-progress variable at 0.7. Filter size $\Delta = 300$ µm. (b) $\langle P^{\star}_{\mathrm{SGS_{EoS}}} | \widetilde{c} \rangle$ with filter size •: $\Delta = 50$ µm, ▲: 100 µm, ♦: 150 µm, ▼: 200 µm, ∘ : 250 µm, +: 300 µm.

and $H_2$ have a negative SGS contribution, reaching -7% and -15%, respectively. Overall, the sign of the SGS term seems to depend on the correlation between the species and the heat release rate (positive for products and negative for reactants). The sum over all species is of the order of -4%.

The pressure variation expected through the laminar flame may be scaled from the conservation of mass and momentum, leading to

$$\frac{\Delta P}{P_{\mathrm{o}}} = \left( \frac{\rho_{\mathrm{o}}}{\rho_{\mathrm{b}}} - 1 \right) \frac{\rho_{\mathrm{o}} S_{\mathrm{L}}^2}{P_{\mathrm{o}}} \,, \tag{4.5}$$

where the subscripts 'o' and 'b' denote fresh and burnt gases, respectively. In accordance with the one-dimensional flame simulation, a variation of the pressure of 0.39% is expected through the $H_2/O_2$ stoichiometric flame (Figure 1(b)). Therefore, the error brought by the linearization of the EoS is of the order of 10 times the flame pressure jump, which would significantly alter the quality of a simulation.

Figure 4(a) shows a snapshot of $(\overline{P} - \overline{\rho} R \widetilde{T} \sum_i (\widetilde{Y}_i / W_i)) / \overline{P}$ in a transverse plane of the slot burner three-dimensional flame for $\Delta = 300$ µm. As in the one-dimensional flame, the normalized SGS contribution peaks at -4%. The amplitude of this SGS part does not seem to be strongly correlated with flame curvature. The mean of the same SGS quantity conditioned on values of the progress variable $\widetilde{c}$, for filter sizes varying between 50 µm and 300 µm, is plotted in Figure 4(b). The progress variable is defined as $\widetilde{c} = \widetilde{Y}_{\mathrm{H_2O}} / Y_{\mathrm{H_2O,b}}$. The amplitude of the conditional mean of the SGS contribution confirms its order of magnitude, which grows with the filter size, with larger values on the fresh gas side (peak at $-2.75\%$ for $\Delta = 300$ µm). The maximum values are also moving toward the reaction zone as the size of the filter increases.

## 5. SGS modeling of the EoS

Equation (2.4) hypothesizes that correlations between temperature and species remain moderate and also that density-weighted averaging could be applied to both $Y_i$ and $T$, even though the density appears only once in the filtered expression. Relaxing the latter

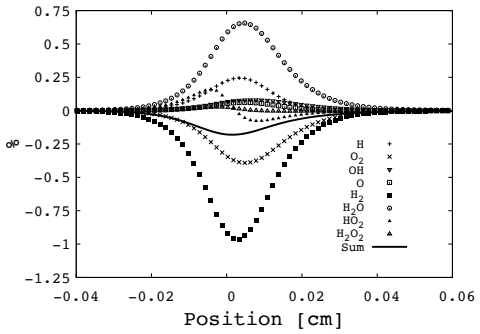


(a) $R(\overline{\rho TY_i} - \overline{\rho}\widetilde{TY}_i)/(W_i\overline{P})$

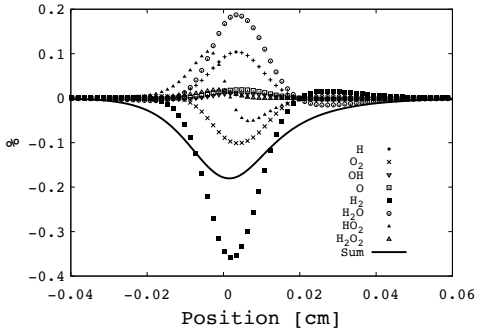


(b) $R(\overline{\rho TY_i} - \overline{\rho}\widetilde{TY}_i - (\overline{\overline{\rho}\widetilde{TY}_i} - \overline{\overline{\rho}}\overline{\widetilde{TY}}_i))/(W_i\overline{P})$

FIGURE 5. Normalized contribution (%) of the $i$-th species and of the sum of the species to the SGS EoS for various formulations. One-dimensional flame *a priori* filtering with filter size $\Delta = 300$ µm.

hypothesis leads to

$$\overline{P} = R\left(\frac{\overline{\rho}\widetilde{TY}_1}{W_1} + \cdots + \frac{\overline{\rho}\widetilde{TY}_n}{W_n}\right) \tag{5.1}$$

where $\overline{Y}_i$ has replaced $\widetilde{Y}_i$. The corresponding normalized SGS term

$$R(\overline{\rho TY_i} - \overline{\rho}\widetilde{TY}_i)/(W_i\overline{P})\,, \tag{5.2}$$

is examined for all species in Figure 5(a) for the one-dimensional flame. The SGS contribution for $H_2O$ and $H_2$ now peaks at 0.66% and 0.96%, respectively. Compared to Figure 3, where 12% and 15% were reported, the reduction brought by the use of Reynolds averaging for the mass fraction is significant. Similarly, the total contribution is reduced to -0.18% with the Reynolds formulation (previously -4%).

To further reduce the departure between the filtered pressure and the pressure computed from filtered quantities, Leonard decomposition may be added to the species and temperature correlations (Germano 1986)

$$\overline{\rho TY_i} - \overline{\rho}\widetilde{TY}_i = \overline{\overline{\rho}\widetilde{TY}_i} - \overline{\overline{\rho}}\overline{\widetilde{TY}}_i + \xi_i\,. \tag{5.3}$$

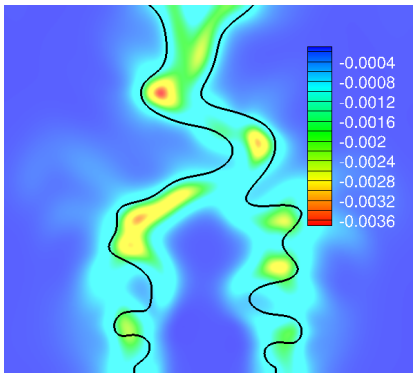


(a) Snapshot in a transverse plane

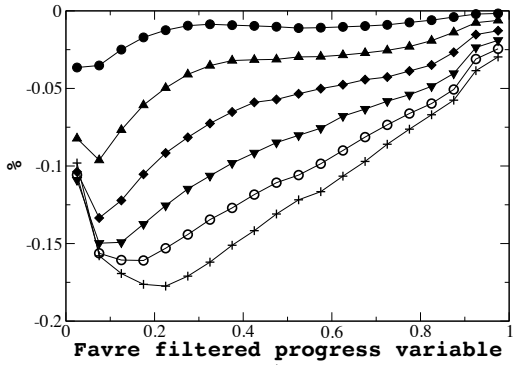


(b) $\left\langle P^{+}_{\mathrm{SGS}_{\mathrm{EoS}}} \middle| \widetilde{c} \right\rangle \times 100$

FIGURE 6. $P^{+}_{\mathrm{SGS}_{\mathrm{EoS}}} = \left(\overline{P} - \overline{\rho} R \widetilde{T} \sum_i (\overline{Y}_i / W_i)\right) / \overline{P}$. 6(b) (a) Black line: iso-progress variable at 0.7. Filter size 300 µm. (b) $\left\langle P^{+}_{\mathrm{SGS}_{\mathrm{EoS}}} \middle| \widetilde{c} \right\rangle \times 100$ with filter size •: $\Delta$ = 50 µm, ▲: 100 µm, ♦: 150 µm, ▼: 200 µm, ∘ : 250 µm, +: 300 µm.

Neglecting the unresolved term $\xi_i$ leads to

$$\overline{P} = R \left( \frac{\overline{\rho}\widetilde{T}\overline{Y}_1 + \overline{\overline{\rho}\widetilde{T}\overline{Y}_1} - \overline{\overline{\rho}}\,\overline{\widetilde{T}\overline{Y}_1}}{W_1} + \cdots + \frac{\overline{\rho}\widetilde{T}\overline{Y}_n + \overline{\overline{\rho}\widetilde{T}\overline{Y}_n} - \overline{\overline{\rho}}\,\overline{\widetilde{T}\overline{Y}_n}}{W_n} \right) . \tag{5.4}$$

Following this modeling, the remaining SGS term

$$R(\overline{\rho T Y_i} - \overline{\rho}\widetilde{T}\overline{Y}_i - (\overline{\overline{\rho}\widetilde{T}\overline{Y}_i} - \overline{\overline{\rho}}\,\overline{\widetilde{T}\overline{Y}_i}))/(W_i\overline{P}) \tag{5.5}$$

is seen for all species across the one-dimensional flame in Figure 5(b). Some SGS terms are further reduced, leading to a peak of 0.18% for $H_2O$ and -0.35% for $H_2$. However, the maximum of the sum over the species is still unchanged at -0.18%. Therefore, for the present case, the compensation of errors over all the species counterbalances the improvement observed for some of them.

Equation (5.1) is thus tested in the three-dimensional flame (i.e., without the Leonard term). Figure 6(a) shows a snapshot of the departure between the filtered pressure and its estimation from Eq. (5.1). Compared to Figure 4(a), which features the usual expression for the pressure, the SGS term that would be neglected is reduced by an order of magnitude. The mean of this term conditioned on the density-weighted progress variable is seen in Figure 6(b), and the same trend is observed in the reduction of the part that would be left unresolved in a simulation. In the three-dimensional turbulent flame, pressure fluctuations associated with large-scale flow motions are observed and the variation of the conditional mean of the pressure between fresh and burnt gases reaches up to 3.5%, which is much larger than that in the one-dimensional laminar flame. This is seen in Figure 7(a) for the conditional mean of the filtered pressure. The conditional mean of the pressure gradient is given in Figure 7(b). The usual expression of the pressure based on the density-weighted filtered mass fraction (dashed line) misses the pressure response in these figures. The use of the Reynolds average (line with circle) captures both the pressure and its gradient.

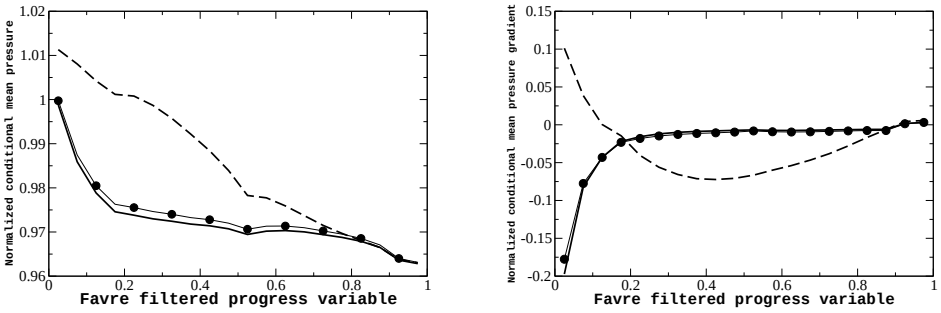


(a) $\langle \overline{P} | \widetilde{c} \rangle / P_o$ (b) $\langle \nabla \overline{P} | \widetilde{c} \rangle / P_o$

FIGURE 7. Conditional mean of pressure and pressure gradient from DNS. ——— : $\overline{P}_{\mathrm{DNS}}$, - - - - : $\overline{P} = \overline{\rho} R \widetilde{T} \sum_i (\widetilde{Y}_i / W_i)$, —●— : $\overline{P} = \overline{\rho} R \widetilde{T} \sum_i (\overline{Y}_i / W_i)$. (a): $\langle \overline{P} | \widetilde{c} \rangle / P_o$. (b): $\langle \nabla \overline{P} | \widetilde{c} \rangle / P_o$.

## 6. Toward LES with SGS modeling of EoS

Equation (5.1), which appears as a valuable expression for the filtered pressure in the case of multicomponent and fully compressible flows, requires the calculation of $\overline{Y}_i$, for which an equation is not solved since density-weighted quantities are usually considered in LES. Relations between $\widetilde{Y}_i$, the transported density weighted mass fractions, and $\overline{Y}_i$, their Reynolds counterpart have been derived in the Reynolds Average Navier Stokes (RANS) literature (Bray 1996). These relations are valid in the asymptotic limit of an infinitely thin flame separating fresh and burnt gases. In LES with complex chemistry, the flame signal must be resolved over the mesh and it cannot be reduced to a jump condition within the sub-grid.

Approximate deconvolution under various conditions has been introduced to estimate unresolved terms from the knowledge of the information available on the mesh nodes (Mathew 2002; Katopodes *et al.* 2004; Bose & Moin 2014; Domingo & Vervisch 2015; Locci & Vervisch 2016). Reversing the approximate Gaussian filtering operation of Eq. (4.3) and applying it to the mesh size $\Delta = \delta_x$ brings an approximate deconvolution operator

$$\rho Y_i = \mathcal{L}_\Delta^{-1}[\overline{\rho}\widetilde{Y}_i] = \overline{\rho}\widetilde{Y}_i - \frac{\delta_x^2}{24}\nabla^2(\overline{\rho}\widetilde{Y}_i)\,; \tag{6.1}$$

then the Reynolds filtered mass fraction reads

$$\overline{Y}_i = \frac{\mathcal{L}_\Delta^{-1}[\overline{\rho}\widetilde{Y}_i]}{\mathcal{L}_\Delta^{-1}[\overline{\rho}]} + \frac{\delta_x^2}{24}\nabla^2\overline{Y}_i\,. \tag{6.2}$$

With this combination of an explicit formulation for deconvolution Eq. (6.1) and an implicit one for filtering (Eq. (6.2)), only derivatives of quantities resolved over the LES mesh are computed, thus avoiding the application of discretization operators to the deconvoluted signals, which may not be fully resolved by the coarse mesh.

This procedure is applied to the one-dimensional flame at first. Figure 8 shows the distribution of the mass fractions (original, density-weigthed filtered, deconvoluted and Reynolds filtered) for the H radical and $\Delta = 300$ μm. The deconvolution at $\Delta$ perfectly recovers the original profiles from the density-weighted mass fraction and thus allows for computing the Reynolds filtered signal, which strongly differs from the density-weighted

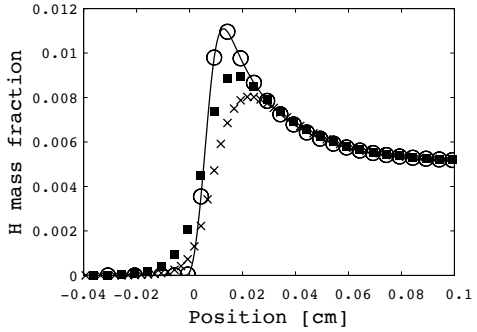


FIGURE 8. One-dimensional flame *a priori* filtering with filter size $\Delta = 300$ µm. ——— : $Y_{\rm H}$. × : $\widetilde{Y}_{\rm H}$. ○ : $Y_{\rm H}$ from deconvolution. ■ : $\overline{Y}_{\rm H}$.

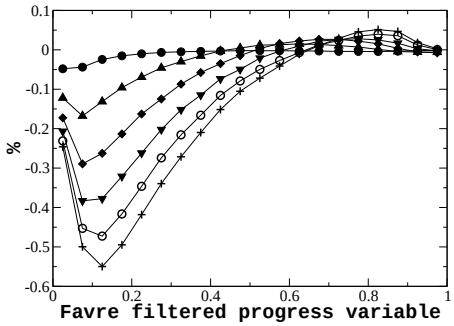


FIGURE 9. $\left\langle 1 - (\overline{\rho}R\widetilde{T}/\overline{P})\sum_i \overline{\mathcal{L}_\Delta^{-1}[\overline{\rho}\widetilde{Y}_i]/(W_i\mathcal{L}_\Delta^{-1}[\overline{\rho}])}\middle|\widetilde{c}\right\rangle$ in %. Filter size •: $\Delta = 50$µm, ▲: 100µm, ♦: 150µm, ▼: 200µm, ○ : 250µm, +: 300µm.

signal in the flame zone. Applied to the three-dimensional flame, the approximate deconvolution/filtering of the density-filtered quantities provides an estimation of the filtered pressure with an error of the order of -0.55% for the larger filter size (Figure 9), which is in line with the direct application of $\overline{Y}_i$ in the EoS reported in Figure 6(b). In this Figure, the departure was of -0.175% at maximum, suggesting that in 3D the deconvolution does not provide $\overline{Y}_i$ values exactly matching the DNS-filtered values. These departures of -0.55% should, however, be compared with the departure of -2.75% observed in Figure 4(b) using the EoS with the density-weighted mass fractions and with the conditional pressure jump between fresh and burnt gases, which is of the order of 3.5% in the turbulent flame (Figure 7(a)).

## 7. Conclusions

The filtering of the EoS, which provides the pressure in fully compressible simulations, has been discussed in the context of oxy-flames for which there is no species dominating the mean molar weight. Two $H_2/O_2$ reacting flows have been examined, including a one-dimensional freely propagating premixed flame and a three-dimensional slot burner

turbulent flame. In both of these flows, *a priori* LES filtering has revealed that the filtered pressure was better approximated using the Reynolds filtered mass fractions of the species to compute the molecular weight of the mixture. A deconvolution procedure has then been set up and evaluated to estimate the Reynolds filtered mass fractions from the density-weighted transported mass fractions.

*Acknowledgments*

Authors have benefited from multiple and fruitful interactions with the members of the CTR Combustion Group. Dr. Pascale Domingo was supported by the project REFINE (ANR-13-BS09-0007).

## REFERENCES

Bose, S. T. & Moin, P. 2014 A dynamic slip boundary condition for wall-modeled large-eddy simulation. *Phys. Fluids.* **26**, 015104.

Bray, K. N. C. 1996 The challenge of turbulent combustion. *Symp. (Int.) Combust.* **26**, 1–26.

Curtiss, C. F. & Hischfelder, J. O. 1949 Transport properties of multicomponent gas mixtures. *J. Chem. Phys.* **17**, 550.

Domingo, P. & Vervisch, L. 2015 Large-eddy simulation of premixed turbulent combustion using approximate deconvolution and explicit flame filtering. *Proc. Combust. Inst.* **35**, 1349–1357.

Ducros, F., Laporte, F., Soulères, T., Guinot, V., Moinat, P. & Caruelle, B. 2000 High-order fluxes for conservative skew-symmetric-like schemes in structured meshes: application to compressible flows. *J. Comput. Phys.* **161**, 114–139.

Germano, M. 1986 A proposal for a redefinition of the turbulent stresses in the filtered Navier-Stokes equation. *Phys. Fluids.* **29**, 2323.

Gottlieb, S. & Shu, C. 1998 Total variation diminishing Runge-Kutta schemes. *Math. Comput.* **67**, 74–85.

Katopodes, F., Street, R. L., Xue, M. & Ferziger, J. H. 2004 Explicit filtering and reconstruction turbulence modeling for large-eddy simulation of neutral boundary layer flow. *J. Atmos. Sci.* **62**, 2058–2077.

Locci, C. & Vervisch, L. 2016 Eulerian scalar projection in Lagrangian point source context: An approximate inverse filtering approach. *Flow Turbul. Combust.* **97**, 363–368.

Lodato, G., Domingo, P. & Vervisch, L. 2008 Three-dimensional boundary conditions for direct and large-eddy simulation of compressible viscous flows. *J. Comput. Phys.* **227**, 5105–5143.

Mathew, J. 2002 Large eddy simulation of a premixed flame with approximate deconvolution modeling. *Proc. Combust. Inst.* **29**, 1995–2000.

Sagaut, P. 2001 *Large Eddy Simulation for Incompressible Flows: An Introduction*, 2nd ed. Berlin Heidelberg: Springer-Verlag.

Selle, L., Okong'o, N., Bellan, J. & Harstad, K. 2007 Modeling of subgrid scale phenomena in supercritical transitional mixing layers: An a priori study. *J. Fluid Mech.* **593**, 57–91.

Williams, F. A. 2008 Detailed and reduced chemistry for hydrogen autoignition. *J. Loss Prevent. Proc.* **21**, 131–135.